




<https://doi.org/10.1038/s42003-025-07797-3>

# Exome sequencing identifies novel genes associated with cerebellar volume and microstructure



Yuanyuan Liang<sup>1,7</sup>, Dongrui Ma<sup>1,7</sup>, Mengjie Li<sup>1</sup>, Zhiyun Wang<sup>1</sup>, Chenwei Hao<sup>1</sup>, Yuemeng Sun<sup>1</sup>, Xiaoyan Hao<sup>1</sup>, Chunyan Zuo<sup>1</sup>, Shuangjie Li<sup>1</sup>, Yanmei Feng<sup>1</sup>, Shasha Qi<sup>1</sup>, Yunpeng Wang<sup>2,3</sup>, Shilei Sun<sup>1,4,5,6</sup>, Yu-Ming Xu<sup>1,4,5,6</sup> , Ole A. Andreassen<sup>2,3</sup>  & Changhe Shi<sup>1,4,5,6</sup> 

Proteins encoded by exons are critical for cellular functions, and mutations in these genes often result in significant phenotypic effects. The cerebellum is linked to various heritable human disease phenotypes, yet genome-wide association studies have struggled to capture the effects of rare variants on cerebellar traits. This study conducts a large-scale exome association analysis using data from approximately 35,000 UK Biobank participants, examining seven cerebellar traits, including total cerebellar volume and white matter microstructure. We identify 90 genes associated with cerebellar traits, 60 of which were previously unreported in genome-wide association studies. Notable findings include the discovery of genes like *PRKRA* and *TTK*, as well as *RASGRP3*, linked to cerebellar volume and white matter microstructure. Gene enrichment analysis reveals associations with non-coding RNA processing, cognitive function, neurodegenerative diseases, and mental disorders, suggesting shared biological mechanisms between cerebellar phenotypes and neuropsychiatric diseases.

Proteins encoded by exons are crucial for cellular functions, and mutations can lead to significant phenotypic effects. The cerebellum, involved in motor and non-motor tasks, is linked to various disease phenotypes and exhibits notable heritability<sup>1–4</sup>. Alterations in cerebellar volume are associated with neurodegenerative disorders, with its white matter microstructure playing a key role in both motor coordination and non-motor functions. These white matter tracts, containing afferent and efferent nerve fibers, facilitate communication with other brain regions and are closely related to neurodegenerative and psychiatric diseases.

Despite previous genome-wide association studies (GWAS) that have identified numerous genetic markers associated with diseases and phenotypes, these studies have primarily focused on common variants (minor allele frequencies (MAF) greater than 1%), which typically exert small effects. Moreover, GWAS often pinpoint disease- or phenotype-associated loci within non-coding regions of the genome, complicating efforts to elucidate molecular disease mechanisms. In contrast, whole-exome sequencing (WES) technology, which concentrates on the

protein-coding regions of the genome, provides an opportunity to explore rare variants that may have been overlooked or inaccurately estimated in traditional GWAS<sup>5</sup>. However, despite WES's potential advantages in understanding disease and phenotype, there remains a paucity of studies utilising large-scale WES data to investigate the cerebellum. Consequently, research employing WES can furnish a more comprehensive understanding of the cerebellum's genetic architecture and provide a scientific foundation for developing strategies to address cerebellum-related diseases.

To our knowledge, the WES analysis conducted in this study represents one of the most extensive investigations of cerebellar genetics to date. Utilising data from the UK Biobank, we performed univariate association tests and gene-based analyses on approximately 35,000 participants. We examined the relationship between genetic variation and both the total volume of the cerebellum and its white matter microstructure, including fractional anisotropy (FA) and mean diffusivity (MD), in the superior, middle and inferior cerebellar peduncles.

<sup>1</sup>Department of Neurology, The First Affiliated Hospital of Zhengzhou University, Zhengzhou University, Zhengzhou, 450000 Henan, China. <sup>2</sup>NORMENT, K.G. Jebsen Centre for Psychosis Research, Institute of Clinical Medicine, University of Oslo, Oslo, Norway. <sup>3</sup>Institute of Clinical Medicine, University of Oslo, Oslo, Norway. <sup>4</sup>NHC Key Laboratory of Prevention and treatment of Cerebrovascular Diseases, The First Affiliated Hospital of Zhengzhou University, Zhengzhou University, Zhengzhou, 450000 Henan, China. <sup>5</sup>Henan Key Laboratory of Cerebrovascular Diseases, The First Affiliated Hospital of Zhengzhou University, Zhengzhou University, Zhengzhou, 450000 Henan, China. <sup>6</sup>Institute of Neuroscience, Zhengzhou University, Zhengzhou, 450000 Henan, China. <sup>7</sup>These authors contributed equally: Yuanyuan Liang, Dongrui Ma. ✉ e-mail: [xuyuming@zzu.edu.cn](mailto:xuyuming@zzu.edu.cn); [ole.andreassen@medisin.uio.no](mailto:ole.andreassen@medisin.uio.no); [shichanghe@gmail.com](mailto:shichanghe@gmail.com)

## Results

### Description of the study population and data

In this study, we utilised phenotypic and genetic data from the UK Biobank, including exome sequencing data and traits associated with the cerebellum (Supplementary Fig. 1). To ensure data quality, we implemented a series of quality control steps on the exome sequencing data to exclude low-quality variants and samples. Our main association analysis included approximately 35,000 White British individuals aged 45–83 years, with 52.91% of the participants being women. The primary cerebellum-related trait of interest was the total volume of the cerebellum. We identified 18,745,074 genetic variants encompassing 160,369 common variants ( $MAF > 1\%$ ) and 18,584,705 rare variants ( $MAF < 1\%$ ). The overall study design is illustrated in Fig. 1.

### Exome-wide association analysis of cerebellum-related traits

To determine the extent to which different types of mutations affect the cerebellum, we assessed the effects of missense mutations and loss-of-function (LOF) variant burdens on cerebellar traits. To further explore the relationship between cerebellar traits and genetic variation, we used SAIGE-GENE+ to calculate associations at the single-variant and gene-based levels (Figs. 2 and 3). Notably, 60 of these genes have not been reported in previous GWAS, highlighting novel genetic insights into cerebellar function. Notably, *PRKRA* and *TTK* emerged from both single-variant and gene-set analyses.

First, we conducted single-variant WES analyses to identify the genetic loci associated with cerebellar traits (Supplementary Data 1, Fig. 2). Using a significance threshold of  $P < 1 \times 10^{-8}$ , we identified 192 genetic associations with cerebellum-related traits, mapping these loci to 81 genes. Among these, 52 genes were newly identified through single-variant analysis, including 14 genes linked to total cerebellar volume and 37 genes associated with white matter microstructure. Notably, *RASGRP3* was associated with cerebellar volume and cerebellar white matter microstructure.

The *PAPPA* gene exhibited the strongest association with total cerebellar volume (chr9:116302764:C:T,  $\beta = 0.1444$ ,  $P = 1.09 \times 10^{-29}$ ), consistent with prior cerebellar GWAS findings. Among the newly discovered genes, *IP6K2* (chr3:48689679:G:A,  $\beta = -0.0442$ ,  $P = 9.99 \times 10^{-11}$ ) showed the strongest association, followed by *ATF7* (chr12:53543094:G:A,  $\beta = 0.0560$ ,  $P = 1.76 \times 10^{-10}$ ). The weakest association after screening was observed for the *QSOX2* gene (chr9:136218808:C:T,  $\beta = 0.0412$ ,  $P = 4.60 \times 10^{-9}$ ). Regarding cerebellar white matter microstructure, 52 genes were identified as significant loci, of which 47 were novel discoveries. Among these, *PPARGC1A* (chr4:2381:T:C,  $\beta = -0.0937$ ,  $P = 1.40 \times 10^{-25}$ ) was most strongly associated with fractional anisotropy of the superior cerebellar peduncle (SCP-FA). *ALDH1A2* was the only gene newly associated with fractional anisotropy of the middle cerebellar peduncle (MCP-FA) (chr15:57960864:C:T,  $\beta = -0.0418$ ,  $P = 7.83 \times 10^{-9}$ ).

Interestingly, the *PPWD1* gene was associated only with SCP-FA in earlier GWAS studies. However, in our analysis, *PPWD1* was also newly associated with fractional anisotropy of the inferior cerebellar peduncle (ICP-FA) (chr5:65569831:T:C,  $\beta = 0.0660$ ,  $P = 9.07 \times 10^{-15}$ ) and mean diffusivity of the superior cerebellar peduncle (SCP-MD) (chr5:65569578:A:G,  $\beta = 0.0752$ ,  $P = 4.98 \times 10^{-21}$ ). Additionally, *TLL1* showed significant associations with both SCP-MD (chr4:166031055:G:A,  $\beta = -0.0859$ ,  $P = 5.53 \times 10^{-19}$ ) and mean diffusivity of the middle cerebellar peduncle (MCP-MD) (chr4:166031055:G:A,  $\beta = -0.0839$ ,  $P = 9.47 \times 10^{-18}$ ) at the same site. For mean diffusivity of the inferior cerebellar peduncle (ICP-MD), the main association was with *PNLDC1* (chr6:159804518:G:C,  $\beta = -0.0631$ ,  $P = 5.61 \times 10^{-11}$ ).

Second, we performed a gene-based analysis considering LOF and missense variants for each gene, with two MAF thresholds ( $<1\%$  and  $<0.1\%$ ). After Bonferroni correction ( $P < 2.5 \times 10^{-6}$ ), we identified eight novel genes significantly associated with cerebellum-related traits, which are presented in the Supplementary Data 2 (Fig. 3). For cerebellar volume, genes such as *SCUBE2* ( $\beta = -0.0077$ ,  $P = 3.25 \times 10^{-7}$ ), *DISP1* ( $\beta = -0.0032$ ,  $P = 1.88 \times 10^{-6}$ ) and *EP300* ( $\beta = 0.0088$ ,  $P = 1.93 \times 10^{-6}$ ) were significantly associated with total cerebellar volume, marking novel discoveries.

Five novel genes were identified for cerebellar white matter microstructure. *PRUNE2* was associated with SCP-FA ( $\beta = -0.0030$ ,  $P = 4.52 \times 10^{-8}$ ) and ICP-FA ( $\beta = -0.0026$ ,  $P = 1.15 \times 10^{-6}$ ). Genes associated with MCP-FA included *TTK* ( $\beta = 0.0047$ ,  $P = 1.05 \times 10^{-7}$ ), *DPYSL2* ( $\beta = -0.1298$ ,  $P = 1.86 \times 10^{-6}$ ) and *C12orf80* ( $\beta = -0.0126$ ,  $P = 1.15 \times 10^{-6}$ ). Additionally, *TTK* ( $\beta = 0.0048$ ,  $P = 2.46 \times 10^{-9}$ ) and *PRKRA* ( $\beta = 0.0146$ ,  $P = 2.83 \times 10^{-10}$ ) were associated with SCP-MD, while *PRKRA* ( $\beta = 0.0132$ ,  $P = 1.35 \times 10^{-8}$ ) was mainly linked to MCP-MD. No significant genes were found for ICP-MD.

Most single variants in the genes identified by the gene-based test showed consistent directional effects, forming a long allele series (Supplementary Data 3). Additionally, the burden of rare variants followed the same direction as the accumulation of each variant. Similar to the GWAS results, we discovered new common genetic loci across the cerebellar white matter tracts, indicating shared genetic factors influencing the white matter tract microstructure.

### Sex analysis

For all identified significant correlations, we conducted a sex sensitivity analysis to assess potential sex-specific effects on cerebellar traits (Supplementary Data 10, 11). Univariate and gene-based analyses were performed separately for male and female participants. The results indicated that the  $\beta$  values of the associations were largely similar to the original values, suggesting consistency across sexes. However, certain genes, such as *AMPD3* and *PAX3*, exhibited stronger associations in females, indicating that sex may influence cerebellar development.

### Conditional analysis

We then conducted conditional analyses to evaluate whether the identified genes were independent of nearby common variants. Initially, we performed a common variant association analysis ( $MAF > 0.5\%$ ) within a  $\pm 500$  kb region surrounding each gene. We then repeated the gene-based folding analysis for the identified genes, incorporating clustered common variants as covariates. Notably, based on the comparison of the conditional analysis results with the original  $p$ -values, the  $p$ -values for *DISP1* and *SCUBE2* remain below 0.05 after conditional analysis, indicating statistical significance. However, the significance and effect size of *DISP1* were diminished, while the  $p$ -value for *SCUBE2* showed no significant change and its effect size remained similar. This suggests that the associations of *SCUBE2* and *DISP1* with rare variants may not be driven by common variants in their vicinity. In contrast, after conditional analysis, the  $p$ -value for *EP300* became non-significant and its effect size decreased, indicating that its association with rare variants might be attributed to more common variants nearby (Supplementary Data 12).

### Burden heritability of cerebellum-related traits

Bayesian Heritability Regression (BHR) is a method for quantifying the heritability explained by the burden of rare coding variants. Weiner et al. demonstrated that rare coding variants account for an average of 1.3% of phenotypic variation<sup>6</sup>. Variants were stratified into bins according to allele frequency and functional class, as suggested by the BHR methodology.

For rare LOF variants, significant non-zero burden heritability was observed in ICP-FA ( $H^2 = 0.32\%$ , S.E. = 0.43%), SCP-MD ( $H^2 = 0.68\%$ , S.E. = 0.48%) and ICP-MD ( $H^2 = 0.80\%$ , S.E. = 0.47%) (Supplementary Data 4, Fig. 4). Compared to the LOF variants, the missense variants showed higher heritability, ranging from 0.12% to 0.87% for the burden of rare variants. The highest heritability was observed for SCP-FA ( $H^2 = 0.87\%$ , S.E. = 0.37%), followed by ICP-FA ( $H^2 = 0.73\%$ , S.E. = 0.40%) and cerebellar volume ( $H^2 = 0.67\%$ , S.E. = 0.28%), with the lowest heritability observed in ICP-MD ( $H^2 = 0.12\%$ , S.E. = 0.33%).

We then used BHR to calculate the genetic correlations between LOF and missense variants across cerebellum-related traits (Supplementary Data 5, Fig. 4). In ICP-MD ( $H^2 = 14.04\%$ , S.E. = 93.29%) and SCP-MD ( $H^2 = 11.18\%$ , S.E. = 78.24%), the LOF and missense variants were

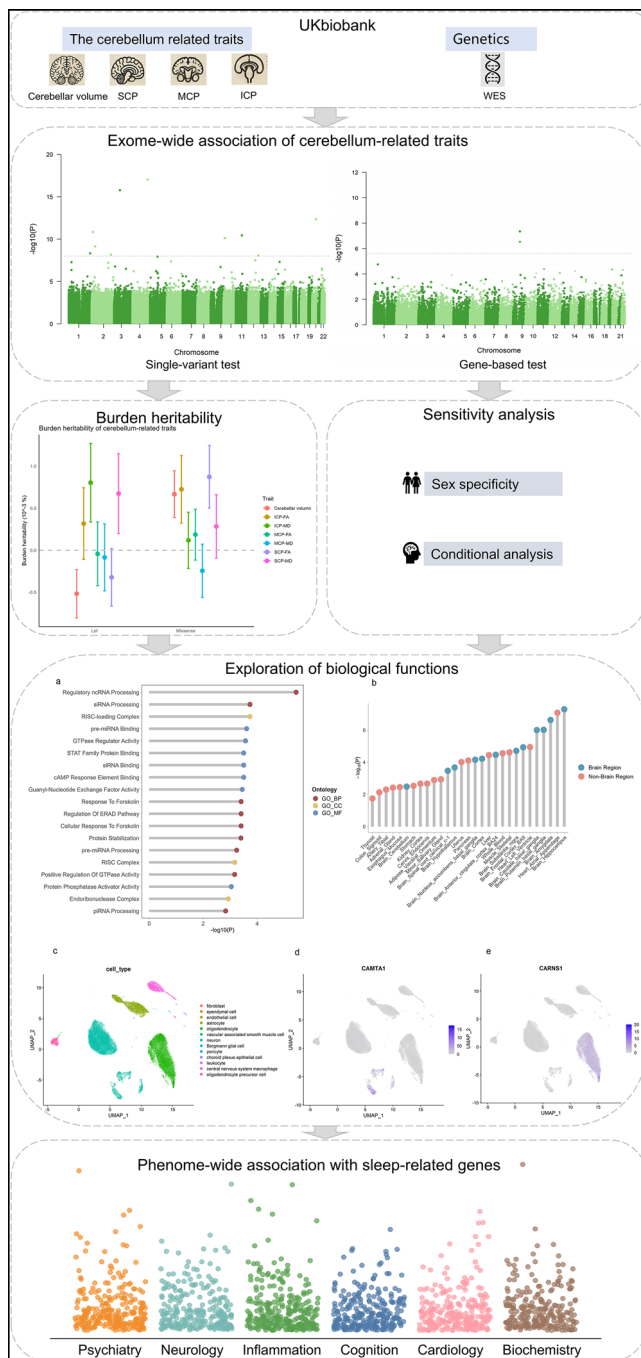


**Fig. 1 | Design of the study.** The analysis utilised cerebellum-related traits and whole exome sequencing data. A whole exome genome-wide association analysis was conducted, including single-variant association tests and gene-based aggregation tests. The workflow incorporated BHR, sex-specific and conditional analyses to explore genetic contributions to cerebellar traits. Biological functions of the identified genes were analysed through GO enrichment, tissue expression profiling and single-cell data analysis. Finally, a PHEWAS was performed to investigate the phenotypic associations of the identified genes.

genetically correlated, suggesting that these variants may have similar phenotypic effects within the same gene in ICP-MD and SCP-MD.

We also estimated rare-variant-burden genetic correlations for different cerebellar traits under the rare variant LOF and missense categories (Supplementary Data 6). The results indicated a substantial genetic correlation between ICP-FA and SCP-MD ( $R_g = 76.89\%$ , S.E. = 61.69%) for rare LOF variants, suggesting a possible shared genetic architecture among these traits. This finding is consistent with the univariate analysis results.

## Biological function of cerebellum-related genes

To characterise the biological properties of the identified genes, we first conducted a pathway enrichment analysis. The Gene Ontology (GO) enrichment analysis revealed that the 54 significant single-variant-associated genes and eight novel genes identified in the gene-based test showed significant enrichment in various biological pathways (Supplementary Data 7, Fig. 5, Supplementary Fig. 2), particularly in non-coding RNA (ncRNA) processing and regulation. Notably, these pathways included regulatory ncRNA processing ( $P = 3.57 \times 10^{-10}$ ) and siRNA processing ( $P = 1.84 \times 10^{-10}$ ). In terms of cell response and signal transduction, the cellular response to forskolin and response to forskolin pathways both exhibited significant enrichment ( $P = 3.92 \times 10^{-10}$ ). For protein degradation and quality control, the regulation of the ERAD pathway was significantly enriched ( $P = 3.92 \times 10^{-10}$ ). Additionally, biological function analysis showed that these genes were significantly enriched in pre-miRNA binding ( $P = 2.45 \times 10^{-10}$ ) and GTPase regulator activity ( $P = 2.69 \times 10^{-10}$ ). Regarding cellular components, the analysis indicated a significant association with the RISC-loading complex ( $P = 1.84 \times 10^{-10}$ ).

We further investigated the expression of the identified genes across different tissues and cell types (Fig. 5). An enrichment analysis of 60 significant genes across 54 tissues from the GTEx project revealed that the top five significantly enriched tissues were Brain – Hippocampus ( $P = 5.01 \times 10^{-10}$ ), Heart – Atrial Appendage ( $P = 8.25 \times 10^{-10}$ ), Brain – Amygdala ( $P = 2.32 \times 10^{-10}$ ), Brain – Substantia nigra ( $P = 9.57 \times 10^{-10}$ ) and Brain – Caudate (basal ganglia) ( $P = 9.92 \times 10^{-10}$ ) (Fig. 5, Supplementary Data 8). Next, we used single-cell RNA sequencing (scRNA-seq) data from the adult cerebellum to explore gene expression in different cell types (Fig. 5, Supplementary Fig. 3). The results showed that *CAMTA1*, *NEBL*, *ADCY8*, *PCNX2*, *DPYSL2*, *PPARGC1A* and *KIAA1109* had significantly higher expression in neuronal cells (Supplementary Fig. 3).

## Phenotypic association with cerebellum-related genes

To explore the association between cerebellum-associated genes and a wide range of phenotypes, we conducted phenotypic association analysis of 60 cerebellum-associated genes identified in single-variant tests (Supplementary Data 9). The phenotypes were categorised into six groups that included 11 behavioural disorders, 10 neurological disorders and six cardiovascular disorders. In our continuous phenotypic analysis, we examined 10 cognitive tasks, 29 blood biochemical characteristics and seven inflammatory indicators.

After correcting for false discovery rate, the phenome-wide association study (PHEWAS) revealed significant associations among the identified genes and phenotypes related to inflammation, biochemistry, cognition, neurodegenerative diseases and behavioural and mental disorders. *RABGAP1L* ( $P = 6.87 \times 10^{-6}$ ) was associated with cognitive function. *IHO1* ( $P = 3.00 \times 10^{-4}$ ) was linked to essential hypertension. *CENPK* ( $P = 7.78 \times 10^{-4}$ ) was associated with persistent delusional disorders. *PRKRA* ( $P = 1.54 \times 10^{-3}$ ) showed a significant association with Parkinson's disease.

## Discussion

In this comprehensive whole-exome analysis, we identified 90 genes significantly associated with seven cerebellar traits, including cerebellar volume and white matter microstructure ( $P < 1 \times 10^{-8}$  for single-variant and  $P < 2.5 \times 10^{-10}$  for gene-based tests). Of these, 60 genes were previously unreported, with shared genetic factors among cerebellar white matter tracts, such as *TTK* and *TLL1*. We replicated 27 genes from previous GWAS, including *PAPPA* and *PPWD1*, and found significant pathway enrichment in neuron-related processes, including non-coding RNA processing. PHEWAS identified associations with neurodegenerative diseases, cognitive function, and mental disorders. Rare LOF variants in ICP-FA explained 76.89% of phenotypic variation, and *SCUBE2* rare variants were linked to cerebellar volume. These findings suggest that rare exon variations

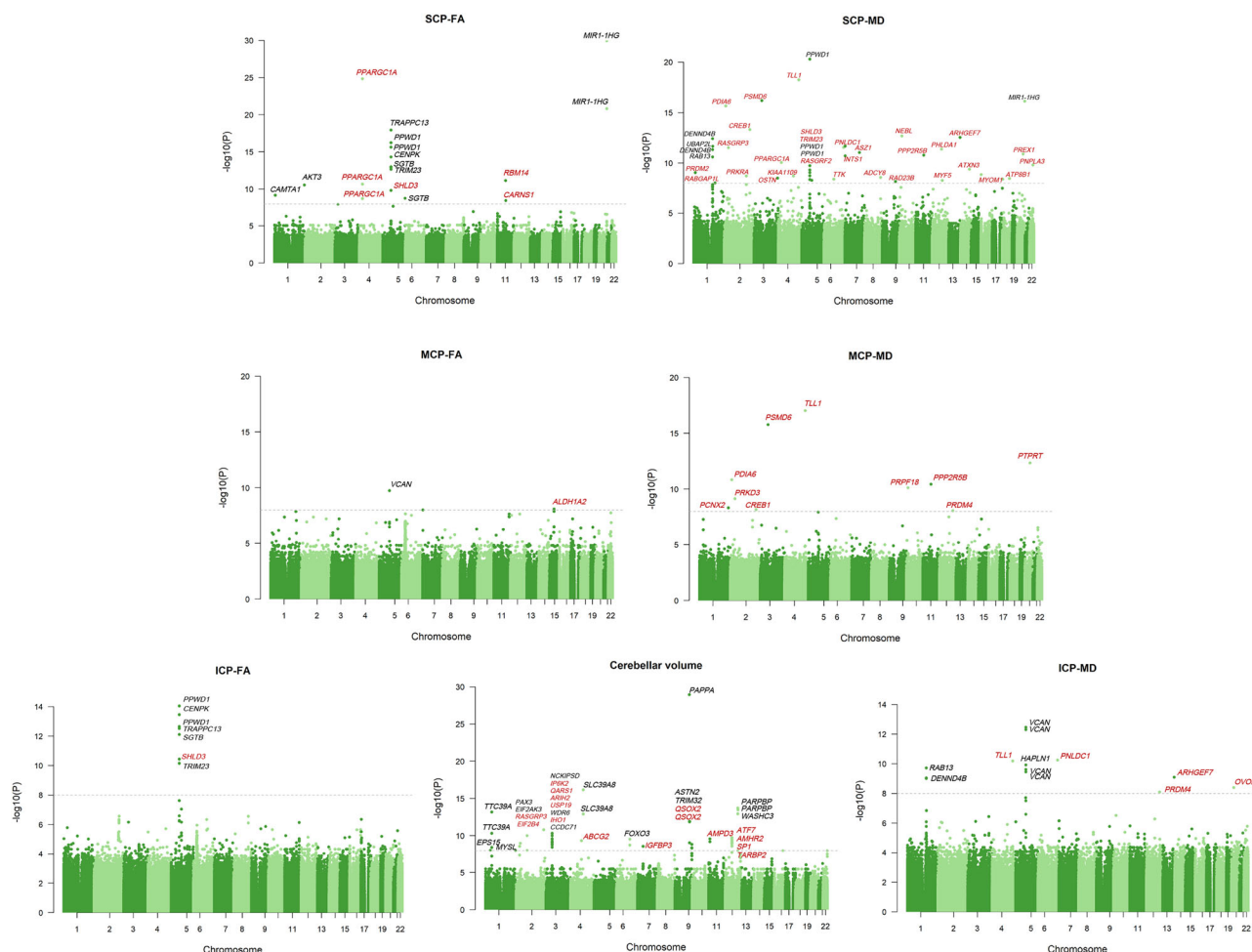


**Fig. 2 | Whole exome genome-wide single-variant tests for cerebellum-related traits.** The Manhattan plot displays the results of single-variant tests associated with cerebellum-related traits, including total cerebellar volume, SCP-FA, SCP-MD, MCP-FA, MCP-MD, ICP-FA and ICP-MD. The x-axis represents the position of

single variants across the 22 chromosomes, while the y-axis indicates the  $-\log_{10} P$ -values for each association. The grey dashed line denotes the significance threshold ( $P < 1 \times 10^{-8}$ ). Variants significantly associated with cerebellum-related traits are labelled with their corresponding genes, with red indicating newly identified genes.

contribute to cerebellar development and share genetic mechanisms with neuropsychiatric diseases, providing insights for potential therapies.

In our single-variant analyses, we extended our understanding of the role of rare variants in cerebellum-related traits beyond previous GWAS that primarily focused on common variants. The genes identified in our study not only play key roles in regulating cerebellar structure and development but are also closely associated with various neuropsychiatric diseases and cognitive dysfunctions.

Specifically, mutations in the *QARS1* gene can lead to protein synthesis disorders that impair the function of cerebellar neurons, resulting in cerebellar atrophy, epilepsy, malformations and early-onset ataxia<sup>7,8</sup>. Similarly, mutations in the *EIF2B4* gene have been clinically linked to cerebellar atrophy and neurodegenerative changes, leading to leukoencephalopathy<sup>9,10</sup>. These findings underscore the cerebellum's critical role in maintaining motor coordination and highlight its high sensitivity to genetic mutations.

The *AMPD3* gene, involved in the adenylate metabolic pathway, is essential for providing sufficient energy supply to the brain, which is crucial for maintaining normal cerebellar function and structure<sup>11,12</sup>. Likewise, the *IGFBP3* gene regulates the biological activity of insulin-like growth factors, potentially influencing cerebellar development and function via the insulin-like growth factor (IGF) pathway and its independent effects<sup>13</sup>. Another gene of interest, *SP1*, is implicated in Alzheimer's disease, whereby functional defects may lead to the accumulation of  $\beta$ -amyloid (A $\beta$ ) and tau proteins, adversely affecting the development and survival of cerebellar

neurons and ultimately causing cerebellar dysfunction<sup>14,15</sup>. Additionally, the *ATF7* gene is associated with the regulation of multiple target genes in the stress response pathway and is linked to schizophrenia and depression<sup>16,17</sup>. In the cerebellum, *ATF7* may play a role in maintaining cerebellar health by regulating neuronal stress responses and structural integrity<sup>18</sup>. The *IP6K2* gene is involved in the phosphoinositide signalling pathway, and its functional defects may result in decreased neuronal survival and reduced cerebellar volume and have a potential impact on cognitive abilities in Alzheimer's disease patients<sup>19–21</sup>. Although there is no direct evidence linking genes such as *ABCG2*, *AMHR2*, *ARIH2*, *USP19*, *RASGRP3*, *IHO1*, *QSOX2* and *TARBP2* to cerebellar volume, these genes may indirectly influence cerebellar volume by affecting neural development and function. Future studies are necessary to further explore the potential roles of these genes.

Among the genes associated with SCP-FA, the *CAMTA1* gene was initially implicated in patients with intragenic deletions and duplications presenting with nonprogressive congecardation, ataxia, behavioural abnormalities and cerebellar anomalies<sup>22</sup>. Furthermore, the *PPARGC1A* gene, which encodes the PGC-1 $\alpha$  protein, is crucial for mitochondrial production and energy metabolism, and its role in cerebellar function and neuroprotection is well documented<sup>23</sup>. Sequence variations in *PPARGC1A* may influence the manifestation of Huntington's disease and contribute to its pathogenesis<sup>24</sup>. While *CARNS1*, *RBM14*, *SHLD3* and *TBC1D9B* do not have direct evidence linking them to cerebellar or other neuropsychiatric diseases, the *ALDH1A2* gene, which encodes aldehyde dehydrogenase, plays



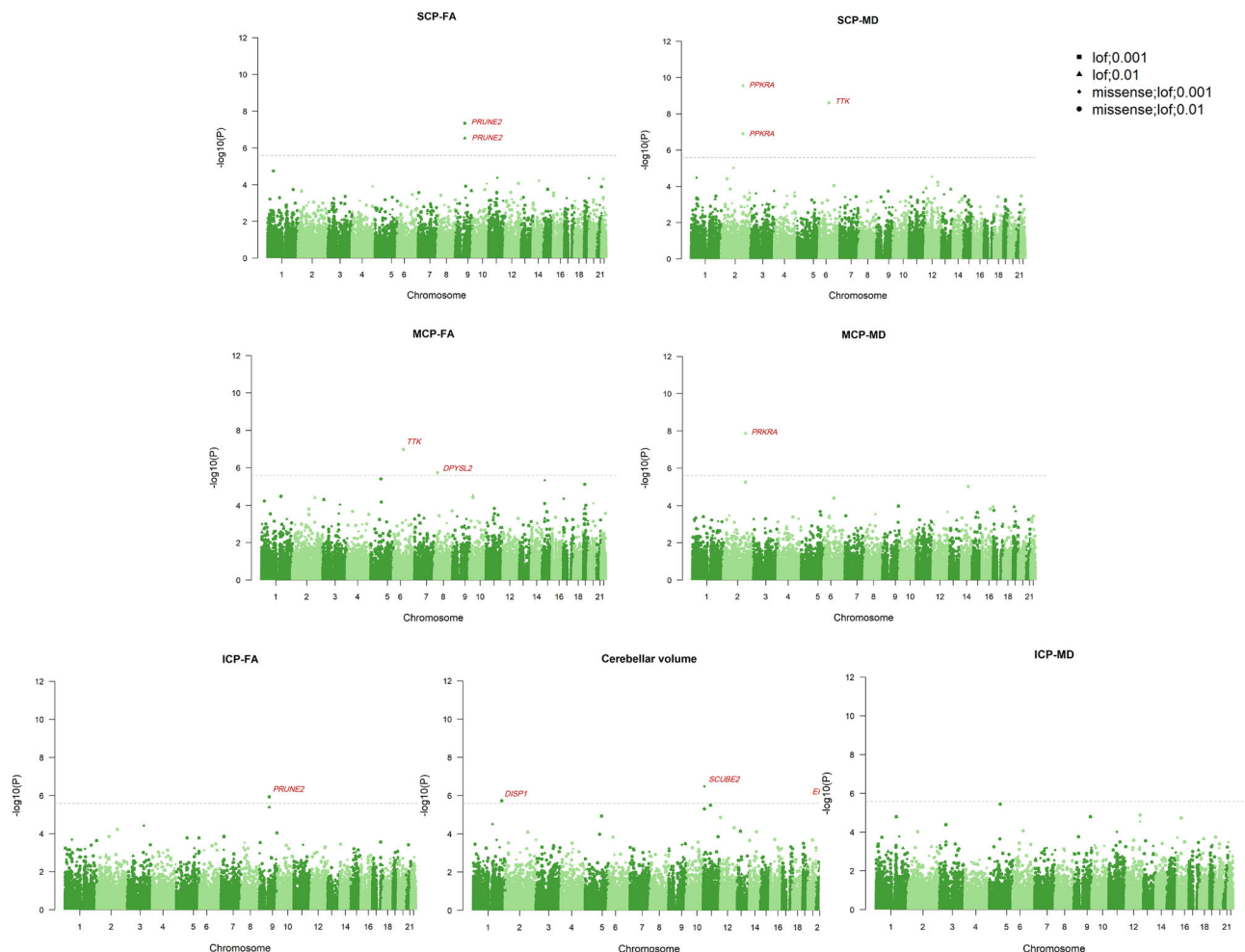


**Fig. 3 | Whole exome genome-wide gene-level tests for cerebellum-related traits.** The Manhattan plot displays the results of gene-level tests associated with cerebellum-related traits, including total cerebellar volume, SCP-FA, SCP-MD, MCP-FA, MCP-MD, ICP-FA and ICP-MD. The gene-level aggregation tests utilised rare variants with two different annotation sets (LOF and LOF + missense) and two

maximum MAF thresholds (1% and 0.1%, respectively). The x-axis represents the position of genes across the 22 chromosomes, while the y-axis indicates the  $-\log_{10} P$ -values for each association. The grey dashed line denotes the significance threshold with Bonferroni correction ( $P < 2.5 \times 10^{-6}$ ). Newly identified genes are highlighted in red.

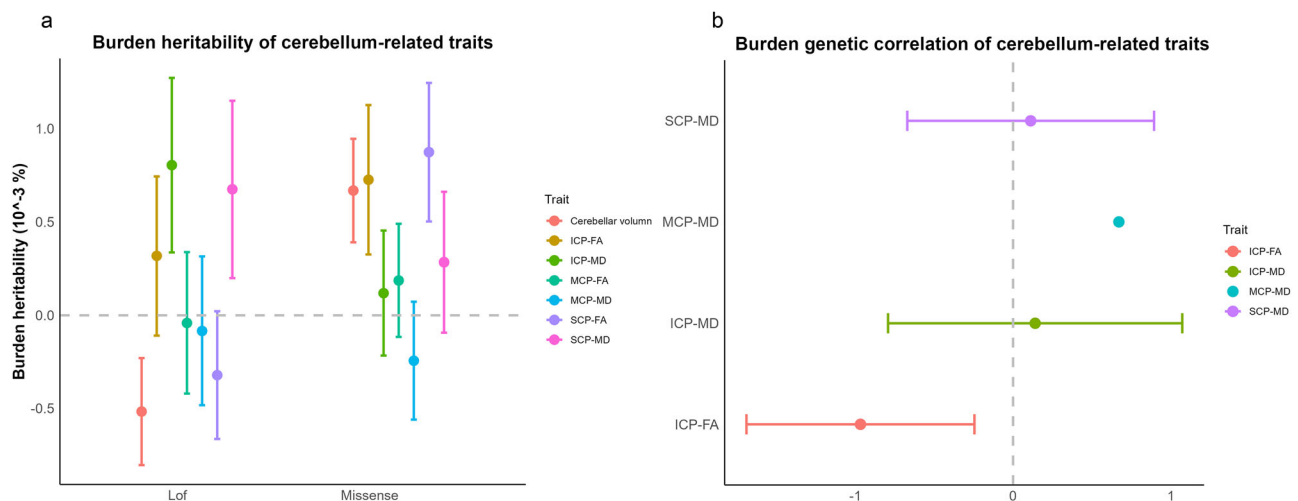


**Fig. 4 | Burden heritability of cerebellum-related traits.** **a** Burden heritability estimates and 95% confidence intervals for rare variants ( $1 \times 10^{-5} \leq \text{MAF} < 1 \times 10^{-3}$ ) in the LOF and missense variant groups. **b** Burden genetic correlation estimates and

95% confidence intervals between LOF and missense variants within rare variant groups. The dashed line indicates a correlation of zero, while the solid line represents the average correlation across all cerebellum-related traits.

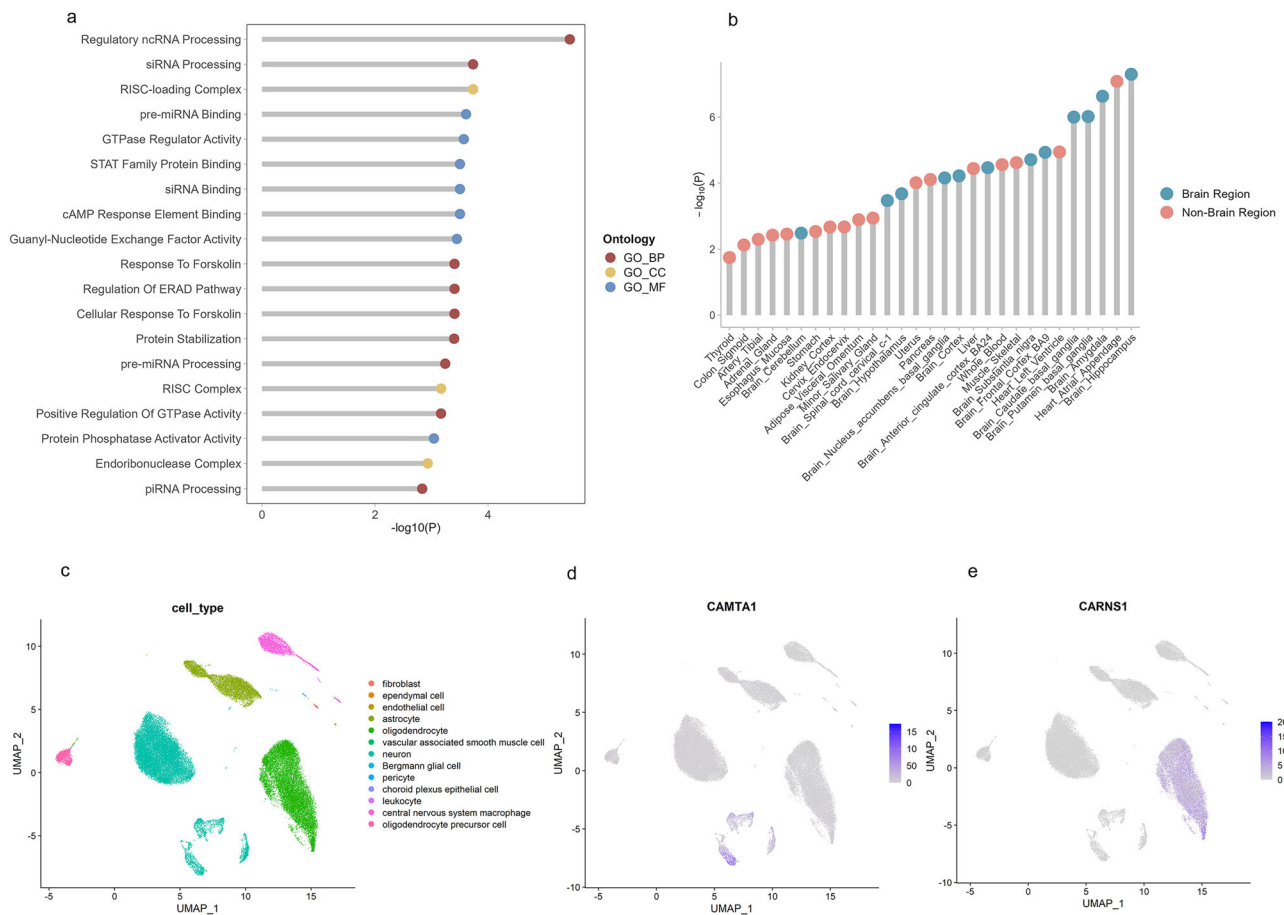


**Fig. 5 | Biological functions of genes associated with cerebellum-related traits.** **a** Enrichment analysis of 60 significant genes identified in single-variant and gene-level tests using the GO database. GO\_BP refers to GO terms from the biological process domain, GO\_CC refers to GO terms from the cellular component domain, and GO\_MF refers to GO terms from the molecular function domain. **b** Enrichment analysis of 68 genes across 54 tissues using FUMA in GTEx. The top 29 tissues are

shown in the figure. **c** Relative expression of cerebellum-associated genes in adult cerebellum single-cell data. Uniform manifold approximation and projection was used to visualise the scRNA-seq data. The colour of each point represents the cell type. **d** Feature plot showing the expression levels of *CAMTA1* across different cell types. **e** Feature plot showing the expression levels of *CARNIS1* across different cell types.

a pivotal role in retinoic acid metabolism in MCP-FA, a process closely associated with neural development<sup>25</sup>. Animal studies have indicated that dysregulation of *ALDH1A2* increases motor neuron vulnerability<sup>26</sup>, and its association with schizophrenia has been observed in Chinese populations<sup>27</sup>, suggesting that *ALDH1A2* and its metabolites may play diverse roles in different neurological diseases. In the context of ICP-FA, the *TRAPPC13* gene has shown significance due to its role in regulating autophagy, which affects cerebellar health<sup>28</sup>. Dysregulation of *TRAPPC13* may contribute to cerebellar autophagy disorders, thereby increasing the risk of neurodegenerative diseases such as Alzheimer's and Parkinson's<sup>15,29</sup>. The *PPWD1* gene, which encodes a protein involved in RNA splicing and pre-mRNA processing, has been associated with SCP-FA in GWAS studies<sup>30</sup>, and our exome analysis suggests that *PPWD1* is also linked to ICP-FA, indicating potential genetic overlap in cerebellar white matter microstructures.

In SCP-MD, mutations in the *ATXN3* gene are known to cause Machado-Joseph disease, or spinocerebellar ataxia type 3, a prevalent inherited ataxia characterised by progressive cerebellar degeneration and motor coordination disorders<sup>31–33</sup>. The *ARHGEF7* and *PREX1* genes are involved in neuronal development and synaptic plasticity, where *ARHGEF7* haploinsufficiency has been linked to epilepsy<sup>34</sup> and *PREX1* may impact cognitive function, particularly in CD4<sup>+</sup> T cells of the elderly<sup>35</sup>. The *CREB1* and *ADCY8* genes are pivotal in memory and learning processes<sup>36–38</sup>, suggesting that disruptions in cerebellar white matter microarchitecture may adversely affect these cognitive functions. Studies on *PRDM2* have proposed that its expression and function in T-cell activation could influence

neuroinflammation<sup>39</sup>, with neuroinflammation caused by immune irregularities impacting cerebellar function and neuropsychiatric health. Furthermore, *KIAA1109* and *RASGRF2* are associated with severe brain development disorders and joint contracture<sup>40</sup>. Recent studies have indicated that disruptions in the *RASGRF2* gene may be a candidate for developmental delay<sup>41</sup>. In the context of MCP-MD and ICP-MD, the *PDIA6* and *PPP2R5B* genes play crucial roles in intracellular protein folding and homeostasis maintenance. *PDIA6* may also contribute to neuroprotection in Alzheimer's disease by regulating the unfolded protein response and protein homeostasis<sup>42,43</sup>. *PRDM4* is mainly involved in transcriptional regulation, and while its specific role in neural development requires further investigation, its importance has been preliminarily acknowledged<sup>44,45</sup>.

To assess the impact of rare genetic variants with a MAF of less than 1% on cerebellum-associated traits, we performed a gene-based analysis and identified eight previously unreported cerebellum-associated genes. Our study confirmed a significant association between *SCUBE2*, *DISP1* and *EP300* with cerebellar volume. However, the conditional analysis suggests that the association of rare variants in *EP300* may be driven by more common variants in its vicinity. Both *SCUBE2* and *DISP1* are involved in regulating the hedgehog signalling pathway. *SCUBE2*, as an extracellular secretory protein, facilitates the diffusion and signal transduction of hedgehog proteins<sup>46</sup>, while *DISP1* is primarily responsible for the extracellular release of hedgehog proteins<sup>47</sup>. Notably, *DISP1* has also been found to potentially influence the response of bipolar disorder to medication, as identified in a GWAS<sup>48</sup>. Mutations in the *EP300* gene have been linked to

Rubinstein–Taybi syndrome (RTS), a rare autosomal dominant disorder characterised by intellectual disability, distinct facial features and cerebellar atrophy<sup>49,50</sup>. Certain mutation types in *EP300*, such as large deletions, are associated with more severe intellectual disabilities and autistic traits<sup>51,52</sup>. Understanding the mechanism of action of *EP300* not only aids in the diagnosis and treatment of RTS but also provides new insights into other neurodevelopmental disorders involving cerebellar function.

In this study, we also found that *PRUNE2*, *DPYSL2*, *C12orf80*, *PRKRA* and *TTK* were significantly associated with cerebellar white matter microstructure. Recent studies have shown that certain variants of *DPYSL2* are associated with an increased risk of schizophrenia, with the gene playing a role in neurodevelopmental disorders through the mTOR signalling pathway<sup>53</sup>. However, the role of *PRUNE2* in schizophrenia has not yet been well defined. *TTK* is known for its role in chromosome segregation and the mitotic checkpoint regulation of cells<sup>54</sup>, with its significance in cell cycle and DNA repair potentially affecting the health and function of cerebellar neurons, thereby influencing global cerebellar function. Currently, functional studies on the *C12orf80* gene are limited, and its potential role in the nervous system needs further exploration. Our analyses, both univariate and gene set-based, revealed significant associations between *PRKRA* and *TTK* with SCP-MD, providing strong evidence for their involvement in cerebellar function. *PRKRA* has been associated with early-onset primary dystonia (DYT-PRKRA)<sup>55</sup>. Recent studies have also discovered that frameshift mutations in the mouse *PRKRA* gene not only result in dystonia but also lead to abnormal cerebellar development and reduced phosphorylation of eIF2 $\alpha$ <sup>56</sup>, suggesting a role for the cerebellum in coordinated movement disorders. These findings offer a new perspective on the role of the cerebellum in psychiatric disorders, indicating that therapies targeting these genes may simultaneously enhance cerebellar function and alleviate psychiatric symptoms, thereby achieving dual therapeutic benefits.

Our study delves deeper into the biomedical mechanisms underlying cerebellar-associated genes. GO pathway enrichment analysis reveals significant associations between these genes and the processing of regulatory non-coding RNAs and small interfering RNAs (siRNAs). Previous research has documented notable alterations in the expression of certain microRNAs (miRNAs), such as miR-223 and miR-124, in neurodegenerative diseases<sup>57–59</sup>. These miRNAs may exert indirect effects on the pathophysiology of cerebellar disorders by modulating key genes involved in neuroinflammation, apoptosis, and neuronal survival. Notably, through the TargetScanHuman 8.0 database, we identified five genes as targets of both miRNAs above (*ARHGEF7*, *PRDM4*, *RABGAP1L*, *SP1*, *TLL1*). The identification of these miRNA-target interactions opens new avenues for further research into how the regulation of these miRNAs could impact cerebellar function, particularly within the context of neurodegenerative diseases. Furthermore, in neurodegenerative disease models, including cerebellar atrophy and Alzheimer’s disease, aberrant siRNA processing disrupts the expression of disease-associated genes. This dysregulation may exacerbate neuronal damage and death, thereby impairing cerebellar function. Thus, abnormal siRNA processing may represent a crucial mechanism by which the cerebellum influences the progression of neurodegenerative diseases. Regarding cellular components, the analysis indicated a significant association with the RISC-loading complex. The RISC-loading complex is a multiprotein complex responsible for loading double-stranded small RNA precursors, such as siRNA or miRNA precursors, onto Argonaute proteins to form mature RNA-induced silencing complex (RISC). Dysfunction in this complex may be linked to neurodegenerative diseases and viral infections.

Our tissue and single-cell expression analysis of the 60 newly identified cerebellum-related genes revealed that these genes are highly expressed in neurons within the nervous system, a finding corroborated by our significant single-cell gene analysis. Beyond their associations with the hippocampus, amygdala and putamen, we also identified a significant relationship between these genes and the heart. In recent years, the physiological connection between the heart and the brain, known as the heart–brain axis, has gained increasing attention. The cardio-cerebral axis

operates through a complex network of autonomic, hormonal and cytokine pathways and plays a vital role in various common diseases<sup>60</sup>. Understanding this mechanism is essential for enhancing prevention and treatment strategies for cardio-cerebral diseases<sup>61</sup>. For instance, Friedreich’s ataxia is an autosomal recessive disorder that affects both the cerebellum, leading to ataxia, and the heart, leading to cardiomyopathy<sup>62,63</sup>. These findings indicate a close relationship between the heart and cerebellum in both health and disease, suggesting that further investigation of these genes may uncover novel therapeutic approaches.

Our study’s strength lies in the large-scale exome analysis of cerebellar volume, combining univariate and gene-based approaches to uncover the genetics underlying cerebellar traits, with further insights from pathway enrichment and PHEWAS analyses into cerebellum-associated neuropsychiatric disorders. However, limitations include reliance on data from White British participants, limiting generalizability to other ethnicities, and the UK Biobank cohort’s bias toward healthy cerebellar features. Additionally, the snRNA-seq analysis, based on postmortem tissue from a small sample ( $n = 3$ ), may be influenced by undiagnosed conditions and lacks detailed clinical data. Larger cohorts and validation in diverse populations, alongside exploration of gene-environment interactions, are needed to confirm the robustness of these findings and enhance their generalizability.

In summary, our study identified 60 novel genes associated with the cerebellum, playing crucial roles in its development and function. Mutations in these genes may link to neuropsychiatric disorders, suggesting a potential cerebellar involvement. The findings also validated associations with cognitive function, neuropsychiatric conditions, inflammation, and biochemical processes. This reveals common biological mechanisms between cerebellar phenotypes and neuropsychiatric diseases, offering insights for future diagnosis and treatment.

## Materials and methods

### Study populations and phenotypes

The UK Biobank is a large prospective cohort study that has collected phenotypic and genetic data from approximately 500,000 participants aged 38–72 years at the time of recruitment. This study received approval from the Northwest Multi-centre Research Ethics Committee, which ensured ethical oversight (<https://www.ukbiobank.ac.uk/learn-more-about-uk-biobank/about-us/ethics>). All ethical regulations relevant to human research participants were followed. Written informed consent was obtained from all participants. The dataset utilised in this analysis included demographic characteristics, cerebellar volume, biochemistry and information on circulatory, cognitive and neuropsychiatric disorders. This study was conducted under application number 104811, 221671. To mitigate the genetic influence of pathological states, we excluded individuals diagnosed with common dementia, stroke and other central nervous system disorders from the analysis (Supplementary Table 1). Cerebellar grey matter and white matter volumes provided by the UK Biobank team were used to calculate total cerebellar volume by summation (Supplementary Table 2). Additionally, we utilised the FA and MD of cerebellar white matter tracts from image-derived phenotypes provided by the UK Biobank. Due to the high genetic correlation of diffusion tensor imaging (DTI) measures between the two hemispheres (all  $R_g > 0.95$ ,  $P < 1 \times 10^{-100}$ ), we averaged the left and right DTI measures for each cerebellar peduncle. Outliers greater than five times the median absolute deviation were removed from all data.

### Exome sequencing and quality control

Exome data were obtained from 454,756 participants in the UK Biobank<sup>64</sup>. The IDT XGEN Exome Research Panel v1.0 was used to capture the exome, and the sequencing scheme is detailed in the relevant literature<sup>5</sup>. In addition to centrally conducted quality control, we implemented comprehensive genotype-, variant- and sample-level quality control procedures, similar to those used in previous studies, to ensure a high-quality dataset<sup>65</sup>.

For genotype quality control, we require at least one heterozygous variant genotype with an allele balance ratio greater than or equal to 15% ( $AB \geq 0.15$ ), and at least one homozygous variant genotype. The same

filtering is applied to INDEL variants, but with an INDEL depth filter of  $DP < 10$  and an INDEL allele balance cutoff of  $AB \geq 0.20$ . Multi-allelic variant sites in the PVCF file are normalized by left-alignment and represented as bi-allelic.

We then perform variant-level quality control and remove variants that fail the following filters: call rate  $< 90\%$ , failed a liberal Hardy–Weinberg Equilibrium (HWE) at  $P < 1 \times 10^{-15}$  among unrelated samples, and monomorphic variants in the final dataset.

For sample quality control, we remove samples with withdrawn consent, duplicate samples, discrepancies between self-reported and genetically inferred sex, as well as unreasonable call rates or additional indicators of poor quality. We compute several quality metrics to identify poor-quality or duplicated samples, using high-quality autosomal variants present in both WES and array datasets to compute per-sample heterozygote concordance rates between WES calls and genotyping array calls. Genetic sex is inferred for each participant using the --check-sex option in PLINK, applying high-quality independent X-chromosomal markers. These markers are selected by excluding pseudo-autosomal regions (bp 2781479 – 155701383), filtering a list of variants in approximate linkage equilibrium using --indep-pairwise with a 200 kilobase window size, 100 step size, and an unphased-hardcall- $r^2$  threshold of 0.05, and excluding call rates of  $< 90\%$ . We also exclude samples that fail a liberal HWE at  $P < 1 \times 10^{-6}$  among unrelated samples.

We also applied the KING-robust algorithm for relatedness filtering (kinship coefficient threshold: 0.0442). Finally, we included approximately 35,000 individuals of White British descent in an all-exome association analysis of cerebellum-related traits.

### Exome-wide association analysis

To identify genetic variants associated with cerebellum-related traits, univariate association tests and gene-based collapse tests were performed using SAIGE-GENE+ software. SAIGE-GENE+ is capable of simultaneously detecting rare and ultra-rare variants, where ultra-rare variants collapse into a single pseudo-marker to reduce data sparsity. For the single-variant association test, we included all variants with a minor allele count (MAC)  $\geq 20$ . In the gene-based collapsing test, we applied two different maximum MAF cutoffs (1% and 0.1%) and two different variant annotation sets LOF and LOF plus missense variants—to perform the SKAT-O test. The correlation coefficient cutoff for the sparse genetic relationship matrix used for variance ratio estimation was set at 0.05.

For cerebellar volume and white matter microstructure analysis, normalisation was employed to adjust for continuous variables. In both the univariate and gene-based collapse tests, models were adjusted for age, sex, body mass index, scanner position parameters (lateral X, transverse Y, longitudinal Z and table position), age squared and the interaction between age squared and sex and the top 10 genetic principal components.

### Sensitivity analysis for sex

For all identified significant correlations, we conducted a sensitivity analysis to examine the influence of sex. We performed univariate association tests and gene-based analyses separately for male and female participants to assess whether the outcomes were affected by sex differences.

### Conditional analysis adjusting for nearby common variation

To determine whether the rare signals identified in the gene-based results were independent of nearby common variants, we performed a secondary gene-based analysis after adjusting for these variants. Initially, we conducted a common variant association analysis ( $MAF > 0.5\%$ ) within a genomic region 500 kb upstream and downstream of each significant gene. For this analysis, we utilised Plink v2.0 (<https://www.coggenomics.org/plink/2.0/>) to conduct genome-wide association analysis using genotype data from UK Biobank v3 imputation. We clustered the results with a cutoff of  $p < 1 \times 10^{-5}$  and  $R^2 < 0.01$ . Subsequently, we reran the gene-based analysis on the identified genes, adjusting for the aggregation of common variants.

Genotype data (version 3) of all 487,409 participants were from the UKB cohort. All blood samples were genotyped using the UK BiLEVE array

and the UK Biobank axion array. Details of the array design, genotyping, quality control, and imputation are available in a previous publication<sup>2</sup>. We performed quality control with PLINK 2.0<sup>3</sup> software. Single-nucleotide polymorphisms (SNPs) with call rates  $< 95\%$ , minor allele frequency  $< 0.1\%$ , and deviation from the Hardy–Weinberg equilibrium with  $P < 1 \times 10^{-50}$  were excluded from the analysis. In addition, samples that were estimated to have no more than ten putative third-degree relatives were included in the analysis.

### Burden heritability and burden genetic correlation

GWAS have identified hundreds of independent loci associated with cerebellar traits and estimated the heritability explained by common variations in the cerebellum to be approximately 0.4–0.5. However, the contribution of rare coding variants to heritability remains unclear. We employed the BHR<sup>6</sup> tool (<https://github.com/ajaynadig/bhr>) to estimate the heritability explained by the gene burden of rare coding variants in cerebellar volume. Variants were stratified into bins based on allele frequency and functional category, as recommended by BHR. Specifically, variants with  $MAF < 1 \times 10^{-5}$  were classified as ultra-rare, while those with  $1 \times 10^{-5} \leq MAF < 1 \times 10^{-3}$  were categorised as rare.

The functionality of each variant was defined according to the ‘Variable Comments’ section of the BHR documentation. All BHR analyses were conducted using the baseline documentation provided by BHR. Univariate BHR analyses were performed to estimate the heritability contribution for cerebellum-related traits, utilising variable-level summary statistics from SAIGE-GENE+ outputs. These statistics were used to obtain effect sizes for quantitative traits directly from the SAIGE-GENE+ results.

### Functional enrichment analysis and tissue expression

We performed an enrichment analysis of 60 genes newly identified in the single-variant association test and the gene-based test. The GO database was selected as the reference for enrichment analysis, dividing GO terms into three categories: biological processes, cellular components and molecular functions. To gain further insight into how these genes influence cerebellar traits, we utilised the Functional Mapping and Annotation (FUMA) tool to examine the enrichment of the 60 genes across 54 different tissues from the Genotype-Tissue Expression (GTEx) project.

### Single-cell expression

For single-cell expression analysis, we utilized publicly available single-cell data from the Human Brain Cell Atlas v1.0, which includes data from the cerebellum of three postmortem donors. Using single-nucleus RNA sequencing (snRNA-seq), we analysed data from cells isolated from the cerebellum comprising 59,236 features and 52,045 cells<sup>66</sup>. We obtained aggregate expression data from the cerebellum and processed it using the R package Seurat. The data were normalised and scaled before clustering and annotation of the scRNA-seq data. Data for this analysis can be accessed via the Human Cell Atlas repository (<https://doi.org/10.1126/science.add7046>).

### Phenome-wide association analysis

We performed a PHEWAS analysis to explore the relationships among genes and various phenotypes (Supplementary Table 3). In the disease analysis, we examined 11 mental and behavioural disorders, 10 neurological disorders and six cardiovascular diseases. For the continuous phenotypic analysis, we investigated 10 cognitive tasks, 29 blood biochemical characteristics and seven inflammatory indicators. The genotype corresponding to the loci identified in the single-variant analysis was used as the exposure variable. We conducted a PHEWAS on the selected phenotypes using the phesant package in R. For newly discovered loci in the single-variant tests, we employed linear or logistic regression models to identify associations between significant variants and phenotypes. All analyses were adjusted for age, sex and the first 10 ancestral principal components.



## Statistics and reproducibility

Statistical analyses were conducted using the R package SAIGE-GENE+ v1.1.6.2 (<https://github.com/saigegit/SAIGE/>), which is capable of detecting rare and ultra-rare variants. Univariate association tests and gene-based collapse tests were performed to identify genetic variants associated with cerebellum-related traits. These tests were adjusted for potential confounding factors, including age, sex, body mass index, scanner position parameters, age squared, and the interaction between age squared and sex, as well as the top 10 genetic principal components.

The sample size for the main association analysis included approximately 35,000 White British individuals from the UK Biobank, aged 45–83 years, with 52.91% women. In total, 18,745,074 genetic variants were analysed, consisting of 160,369 common variants (minor allele frequency >1%) and 18,584,705 rare variants (minor allele frequency <1%).

For single-cell expression analysis, publicly available single-cell RNA sequencing data from the Human Brain Cell Atlas v1.0 were utilized. The dataset included data from three postmortem donors' cerebellum (<https://doi.org/10.1126/science.add7046>), consisting of 52,045 cells and 59,236 features. The data were processed using Seurat v4.3.0 (<https://github.com/satijalab/seurat/>), and normalized, scaled, and clustered before annotation.

Data quality control (QC) was performed using Hail (<https://hail.is>) and PLINK v2.0 (<https://www.cog-genomics.org/plink/2.0/>). Genotype QC involved removal of variants with call rates <90%, variants failing the Hardy–Weinberg equilibrium test ( $P < 1 \times 10^{-15}$ ), and monomorphic variants. We also applied the KING-robust algorithm for relatedness filtering (kinship coefficient threshold: 0.0442). Outliers were removed if they exceeded five times the median absolute deviation (MAD). Sensitivity analysis was performed to examine the impact of genotype-derived sex by conducting separate univariate association tests and gene-based analyses for male and female participants.

Replicates were defined as independent samples from individuals with similar demographic characteristics, analyzed separately to ensure consistency in the results. All analyses were conducted with the assumption that the data would be reproducible using the same methods and datasets.

## Reporting summary

Further information on research design is available in the Nature Portfolio Reporting Summary linked to this article.

## Data availability

The primary data used in this study, including individual-level phenotypic and genetic data, were obtained from the UK Biobank under application numbers 104811 and 221671. These data are accessible through the UK Biobank portal (<https://www.ukbiobank.ac.uk/>). Additionally, single-cell sequencing data for the adult cerebellum were sourced from the Human Brain Cell Atlas v1.0, which includes data from three postmortem donors (<https://doi.org/10.1126/science.add7046>, <https://data.humancellatlas.org/hca-bio-networks/nervous-system/atlas/brain-v1-0>). Source data for all figures can be found in Supplementary Data 1, 2, 4, 5, 6, 7, and 8.

## Code availability

The code used for single-variant and gene-based analyses was from the R package SAIGE-GENE+ v1.1.6.2 (<https://github.com/saigegit/SAIGE/>). Quality control (QC) of individual-level data was conducted using Hail (<https://hail.is>) and PLINK v2.0 (<https://www.cog-genomics.org/plink/2.0/>). Variant annotation was performed using SnpEff v5.1 (<https://pcingola.github.io/SnpEff/>). Load heritability estimation was performed using BHR v0.1.0 (<https://github.com/ajaynadig/bhr/>). Analysis and visualization of scRNA-seq data were conducted using Seurat v4.3.0 (<https://github.com/satijalab/seurat/>). GO enrichment analysis was performed using ClusterProfiler v4.2.2 (<https://maayanlab.cloud/Enrichr/>). Tissue expression enrichment analysis was conducted using FUMA v1.5.6 (<https://fuma.ctglab.nl/>).

Received: 28 September 2024; Accepted: 21 February 2025;

Published online: 01 March 2025

## References

- Kozioł, L. F. et al. Consensus paper: the cerebellum's role in movement and cognition. *Cerebellum* **13**, 151–177 (2014).
- Kozioł, L. F., Budding, D. E. & Chidekel, D. From movement to thought: executive function, embodied cognition, and the cerebellum. *Cerebellum* **11**, 505–525 (2012).
- Baumann, O. & Mattingley, J. B. Cerebellum and Emotion Processing. *Adv. Exp. Med. Biol.* **1378**, 25–39 (2022).
- Schmahmann, J. D., Guell, X., Stoodley, C. J. & Halko, M. A. The Theory and Neuroscience of Cerebellar Cognition. *Annu Rev. Neurosci.* **42**, 337–364 (2019).
- Van Hout, C. V. et al. Exome sequencing and characterization of 49,960 individuals in the UK Biobank. *Nature* **586**, 749–756 (2020).
- Weiner, D. J. et al. Polygenic architecture of rare coding variation across 394,783 exomes. *Nature* **614**, 492–499 (2023).
- Zhang, X. et al. Mutations in QARS, encoding glutamyl-tRNA synthetase, cause progressive microcephaly, cerebral-cerebellar atrophy, and intractable seizures. *Am. J. Hum. Genet.* **94**, 547–558 (2014).
- Kodera, H. et al. Mutations in the glutamyl-tRNA synthetase gene cause early-onset epileptic encephalopathy. *J. Hum. Genet.* **60**, 97–101 (2015).
- Wei, C. et al. Adult-onset vanishing white matter disease with the EIF2B2 gene mutation presenting as menometrorrhagia. *BMC Neurol.* **19**, 203 (2019).
- Tian, Y. et al. Identification of a Novel Heterozygous Mutation in the EIF2B4 Gene Associated With Vanishing White Matter Disease. *Front. Bioeng. Biotechnol.* **10**, 901452 (2022).
- Chang, C.-P., Wu, K.-C., Lin, C.-Y. & Chern, Y. Emerging roles of dysregulated adenosine homeostasis in brain disorders with a specific focus on neurodegenerative diseases. *J. Biomed. Sci.* **28**, 70 (2021).
- Watts, M. E., Pocock, R. & Claudianos, C. Brain energy and oxygen metabolism: emerging role in normal function and disease. *Front. Mol. Neurosci.* **11**, 216 (2018).
- Varma Shrivastav, S., Bhardwaj, A., Pathak, K. A. & Shrivastav, A. Insulin-Like Growth Factor Binding Protein-3 (IGFBP-3): Unraveling the Role in Mediating IGF-Independent Effects Within the Cell. *Front. Cell Dev. Biol.* **8**, 286 (2020).
- d'Errico, P. & Meyer-Luehmann, M. Mechanisms of Pathogenic Tau and Aβ Protein Spreading in Alzheimer's Disease. *Front. Aging Neurosci.* **12**, <https://doi.org/10.3389/fnagi.2020.00265> (2020).
- Jacobs, H. I. L. et al. The cerebellum in Alzheimer's disease: evaluating its role in cognitive decline. *Brain* **141**, 37–47 (2017).
- Welcome, M. O. Cellular mechanisms and molecular signaling pathways in stress-induced anxiety, depression, and blood–brain barrier inflammation and leakage. *Inflammopharmacology* **28**, 643–665 (2020).
- Jiang, S., Postovit, L., Cattaneo, A., Binder, E. B. & Aitchison, K. J. Epigenetic Modifications in Stress Response Genes Associated With Childhood Trauma. *Front. Psychiatry* **10**, <https://doi.org/10.3389/fpsyt.2019.00808> (2019).
- Fletcher, M., Tillman, E. J., Butty, V. L., Levine, S. S. & Kim, D. H. Global transcriptional regulation of innate immunity by ATF-7 in *C. elegans*. *PLoS Genet* **15**, e1007830 (2019).
- Razani, E. et al. The PI3K/Akt signaling axis in Alzheimer's disease: a valuable target to stimulate or suppress? *Cell Stress Chaperones* **26**, 871–887 (2021).
- Kumar, M. & Bansal, N. Implications of Phosphoinositide 3-Kinase-Akt (PI3K-Akt) Pathway in the Pathogenesis of Alzheimer's Disease. *Mol. Neurobiol.* **59**, 354–385 (2022).

21. Limantoro, J., de Liyis, B. G. & Sutedja, J. C. Akt signaling pathway: a potential therapy for Alzheimer's disease through glycogen synthase kinase 3 beta inhibition. *Egypt. J. Neurol. Psychiatry Neurosurg.* **59**, 147 (2023).
22. Shinawi, M., Coorg, R., Shimony, J. S., Grange, D. K. & Al-Kateb, H. Intragenic CAMTA1 deletions are associated with a spectrum of neurobehavioral phenotypes. *Clin. Genet* **87**, 478–482 (2015).
23. Chen, M. et al. The Role of PGC-1 $\alpha$ -Mediated Mitochondrial Biogenesis in Neurons. *Neurochem. Res.* **48**, 2595–2606 (2023).
24. Taherzadeh-Fard, E. et al. PGC-1 $\alpha$  downstream transcription factors NRF-1 and TFAM are genetic modifiers of Huntington disease. *Mol. Neurodegeneration* **6**, 32 (2011).
25. Leon, E., Nde, C., Ray, R. S., Preciado, D. & Zohn, I. E. ALDH1A2-related disorder: A new genetic syndrome due to alteration of the retinoic acid pathway. *Am. J. Med Genet A* **191**, 90–99 (2023).
26. Kataoka, M. et al. Dysregulation of Aldh1a2 underlies motor neuron degeneration in spinal muscular atrophy. *Neurosci. Res.* **194**, 58–65 (2023).
27. Wan, C. et al. Positive association between ALDH1A2 and schizophrenia in the Chinese population. *Prog. Neuropsychopharmacol. Biol. Psychiatry* **33**, 1491–1495 (2009).
28. Ramírez-Peinado, S. et al. TRAPPC13 modulates autophagy and the response to Golgi stress. *J. Cell Sci.* **130**, 2251–2265 (2017).
29. Krajcovicova, L., Klobusiakova, P. & Rektorova, I. Gray Matter Changes in Parkinson's and Alzheimer's Disease and Relation to Cognition. *Curr. Neurol. Neurosci. Rep.* **19**, 85 (2019).
30. Wu, B. S. et al. Genome-wide association study of cerebellar white matter microstructure and genetic overlap with common brain disorders. *Neuroimage* **269**, 119928 (2023).
31. Paulson, H. Machado-Joseph disease/spinocerebellar ataxia type 3. *Handb. Clin. Neurol.* **103**, 437–449 (2012).
32. Dulski, J. et al. Spinocerebellar ataxia type 3 (Machado-Joseph disease). *Pol. Arch. Intern. Med.* **132**, <https://doi.org/10.20452/pamw.16322> (2022).
33. Colomer Gould, V. F. Mouse models of spinocerebellar ataxia type 3 (Machado-Joseph disease). *Neurotherapeutics* **9**, 285–296 (2012).
34. Orsini, A. et al. Generalized epilepsy and mild intellectual disability associated with 13q34 deletion: A potential role for SOX1 and ARHGEF7. *Seizure* **59**, 38–40 (2018).
35. Zhang, H. et al. PREX1 improves homeostatic proliferation to maintain a naive CD4<sup>+</sup> T cell compartment in older age. *JCI Insight* **9**, <https://doi.org/10.1172/jci.insight.172848> (2024).
36. Kandel, E. R. The molecular biology of memory: cAMP, PKA, CRE, CREB-1, CREB-2, and CPEB. *Mol. Brain* **5**, 14 (2012).
37. Pramio, D. T. et al. DNA methylation of the promoter region at the CREB1 binding site is a mechanism for the epigenetic regulation of brain-specific PKM $\zeta$ . *Biochim. Biophys. Acta Gene Regul. Mech.* **1866**, 194909 (2023).
38. Zhang, M. & Wang, H. Ca(2<sup>+</sup>)-stimulated ADCY1 and ADCY8 regulate distinct aspects of synaptic and cognitive flexibility. *Front. Cell Neurosci.* **17**, 1215255 (2023).
39. Di Zazzo, E. et al. Exploring the putative role of PRDM1 and PRDM2 transcripts as mediators of T lymphocyte activation. *J. Transl. Med.* **21**, 217 (2023).
40. Gueneau, L. et al. KIAA1109 Variants Are Associated with a Severe Disorder of Brain Development and Arthrogryposis. *Am. J. Hum. Genet* **102**, 116–132 (2018).
41. Lederbogen, R. C. et al. Optical Genome Mapping Reveals Disruption of the RASGRF2 Gene in a Patient with Developmental Delay Carrying a De Novo Balanced Reciprocal Translocation. *Genes* **15**, <https://doi.org/10.3390/genes15060809> (2024).
42. Hetz, C. & Mollereau, B. Disturbance of endoplasmic reticulum proteostasis in neurodegenerative diseases. *Nat. Rev. Neurosci.* **15**, 233–249 (2014).
43. Xu, J. et al. Human striatal glia differentially contribute to AD- and PD-specific neurodegeneration. *Nat. Aging* **3**, 346–365 (2023).
44. Hohenauer, T. & Moore, A. W. The Prdm family: expanding roles in stem cells and development. *Development* **139**, 2267–2282 (2012).
45. Bogani, D. et al. The PR/SET domain zinc finger protein Prdm4 regulates gene expression in embryonic stem cells but plays a nonessential role in the developing mouse embryo. *Mol. Cell Biol.* **33**, 3936–3950 (2013).
46. Lin, Y.-C., Sahoo, B. K., Gau, S.-S. & Yang, R.-B. The biology of SCUBE. *J. Biomed. Sci.* **30**, 33 (2023).
47. Zhang, Y. & Beachy, P. A. Cellular and molecular mechanisms of Hedgehog signalling. *Nat. Rev. Mol. Cell Biol.* **24**, 668–687 (2023).
48. Ho, A. M. et al. Mood-Stabilizing Antiepileptic Treatment Response in Bipolar Disorder: A Genome-Wide Association Study. *Clin. Pharm. Ther.* **108**, 1233–1242 (2020).
49. Lacombe, D. et al. Diagnosis and management in Rubinstein-Taybi syndrome: first international consensus statement. *J. Med Genet* **61**, 503–519 (2024).
50. Sima, A. et al. Menke-Hennekam Syndrome: A Literature Review and a New Case Report. *Children* **9**, <https://doi.org/10.3390/children9050759> (2022).
51. López, M. et al. Rubinstein-Taybi 2 associated to novel EP300 mutations: deepening the clinical and genetic spectrum. *BMC Med. Genet.* **19**, 36 (2018).
52. Van Gils, J., Magdinier, F., Fergelot, P. & Lacombe, D. Rubinstein-Taybi Syndrome: A Model of Epigenetic Disorder. *Genes* **12**, <https://doi.org/10.3390/genes12070968> (2021).
53. Feuer, K. L., Peng, X., Yovo, C. K. & Avramopoulos, D. DPYSL2/CRMP2 isoform B knockout in human iPSC-derived glutamatergic neurons confirms its role in mTOR signaling and neurodevelopmental disorders. *Mol. Psychiatry* **28**, 4353–4362 (2023).
54. Pachis, S. T. & Kops, G. Leader of the SAC: molecular mechanisms of Mps1/TTK regulation in mitosis. *Open Biol.* **8**, <https://doi.org/10.1098/rsob.180109> (2018).
55. Thomsen, M., Lange, L. M., Zech, M. & Lohmann, K. Genetics and Pathogenesis of Dystonia. *Annu Rev. Pathol.* **19**, 99–131 (2024).
56. Burnett, S. B. et al. A frameshift mutation in the murine Prkra gene causes dystonia and exhibits abnormal cerebellar development and reduced eIF2 $\alpha$  phosphorylation. *bioRxiv*, <https://doi.org/10.1101/2024.06.04.597421> (2024).
57. Harraz, M. M., Eacker, S. M., Wang, X., Dawson, T. M. & Dawson, V. L. MicroRNA-223 is neuroprotective by targeting glutamate receptors. *Proc. Natl. Acad. Sci. USA* **109**, 18962–18967 (2012).
58. Nelson, P. T. & Wang, W. X. MiR-107 is reduced in Alzheimer's disease brain neocortex: validation study. *J. Alzheimers Dis.* **21**, 75–79 (2010).
59. Ambasudhan, R. et al. Direct reprogramming of adult human fibroblasts to functional neurons under defined conditions. *Cell Stem Cell* **9**, 113–118 (2011).
60. Hu, J.-R., Abdullah, A., Nanna, M. G. & Soufer, R. The Brain-Heart Axis: Neuroinflammatory Interactions in Cardiovascular Disease. *Curr. Cardiol. Rep.* **25**, 1745–1758 (2023).
61. Villringer, A. & Laufs, U. Heart failure, cognition, and brain damage. *Eur. Heart J.* **42**, 1579–1581 (2021).
62. Zesiewicz, T. A. et al. Emerging therapies in Friedreich's Ataxia. *Expert Rev. Neurother.* **20**, 1215–1228 (2020).
63. Krasilnikova, M. M., Humphries, C. L. & Shinsky, E. M. Friedreich's ataxia: new insights. *Emerg. Top. Life Sci.* **7**, 313–323 (2023).
64. Backman, J. D. et al. Exome sequencing and analysis of 454,787 UK Biobank participants. *Nature* **599**, 628–634 (2021).
65. Jurgens, S. J. et al. Analysis of rare genetic variation underlying cardiometabolic diseases and traits among 200,000 individuals in the UK Biobank. *Nat. Genet* **54**, 240–250 (2022).
66. Siletti, K. et al. Transcriptomic diversity of cell types across the adult human brain. *Science* **382**, eadd7046 (2023).

